



Seismicity and earthquake focal mechanisms in North-Western Croatia

Davorka Herak^a, Marijan Herak^{a,*}, Bruno Tomljenović^b

^a University of Zagreb, Faculty of Science and Mathematics, Department of Geophysics, Zagreb, Horvatovac bb, 10000 Zagreb, Croatia

^b University of Zagreb, Faculty of Mining, Geology and Petroleum Engineering, Zagreb, Croatia

ARTICLE INFO

Article history:

Received 3 April 2008

Received in revised form 25 November 2008

Accepted 4 December 2008

Available online 10 December 2008

Keywords:

Seismicity

Catalogue completeness

Fault-plane solutions

Pannonian basin

Croatia

ABSTRACT

The seismicity of NW Croatia, seismically the most vulnerable part of the country is presented based on historical records and reanalysed and relocated earthquakes occurring after 1908. The improved picture of the distribution of seismicity shows consistent grouping of foci in space, mostly within eight epicentral areas. The database of fault-plane solutions has been considerably enlarged, and now lists 22 earthquakes. The earthquake mechanisms consistently reveal the subhorizontal to moderately dipping *P*-axis, predominantly N–S directed in the central part of studied area, to NW–SE and NE–SW directed in the western and eastern parts, respectively. They indicate the prevalence of compressional tectonics with reverse faulting in the central part versus strike-slip motions in the western and eastern sectors. These data are in agreement with stress calculations and kinematics of Quaternary structures obtained by geological studies. The completeness of the catalogue, estimated by comparing the cumulative activity rate for a large number of subcatalogues to the reference, contemporary rate, exhibits large spatial heterogeneity. Taking this into account, we have computed and mapped the parameters of the frequency-magnitude recurrence relation (the *b*-value and the activity rate).

© 2008 Elsevier B.V. All rights reserved.

1. Introduction

Seismicity of NW Croatia can be characterized as moderate with rare occurrences of strong events, both features typical for regions of intraplate seismicity. Although not the most earthquake-prone region in Croatia, it is seismically the most vulnerable one due to its economic importance and concentration of population centres including the capital, Zagreb. It covers about 30% of the total country area, with 45% of the population and over 55% of the national product. Tectonically, it lies in the border zone between the Alps, the Dinarides and the Pannonian basin, at the “triple junction” between the Periadriatic, Balaton and Drava transcurrent faults, all playing important role in the Neogene–Quaternary tectonics in this and the surrounding region (e.g. Fodor et al., 1998; Prelogović et al., 1998; Tomljenović and Csontos, 2001; Tomljenović et al., 2008). Particular segments of these faults and their accompanying splays have been proven as Quaternary active structures potentially capable of generating moderate to strong earthquakes (e.g. Prelogović et al., 1998; Magyari et al., 2005). In spite of this, the seismicity of NW Croatia has not been studied in detail yet. Only parts of it were briefly described by Prelogović et al. (1998), and the overall activity was presented within periodical reports on Croatian seismicity by Herak et al. (1991), Markušić et al.

(1993, 1998), and Ivančić et al. (2002, 2006). All data on earthquakes—the catalogues, macroseismic reports, seismograms, and other related documents—are taken from the archives of the Department of Geophysics, Faculty of Science and Mathematics, University of Zagreb. The Croatian Earthquake Catalogue (CEC), covering the period since 373 BC until today, is the primary source of information. Its first revision was described by Herak et al. (1996). Ever since, the catalogue has been regularly updated, so that it currently reports the basic data on over 30,000 events with foci in Croatia and the neighbouring regions.

The area investigated in this paper is bounded by the coordinates 15.25–17.70°E and 45.35–46.55°N (Fig. 1). In general, seismicity of NW Croatia is unevenly distributed and is mostly related to eight epicentral areas. The most active ones lie along its northern and western margins. Strong events have also occurred in the southern part, including the famous Kupa Valley earthquake of 1909, the analyses of which led A. Mohorovičić to the discovery of the crust–mantle boundary in 1910. Seismicity of the central and eastern parts is rather low.

2. Relocation of the instrumentally recorded earthquakes

The Croatian Earthquake Catalogue is routinely updated (as a rule 3–4 times a year) with hypocentral locations and magnitudes obtained through a semi-automatic location procedure. Using all read onset times of various local and regional phases from Croatian stations, as well as those reported by other regional networks at the

* Corresponding author. Tel.: +385 1 4605 914; fax: +385 1 4680 331.
E-mail address: herak@irb.hr (M. Herak).

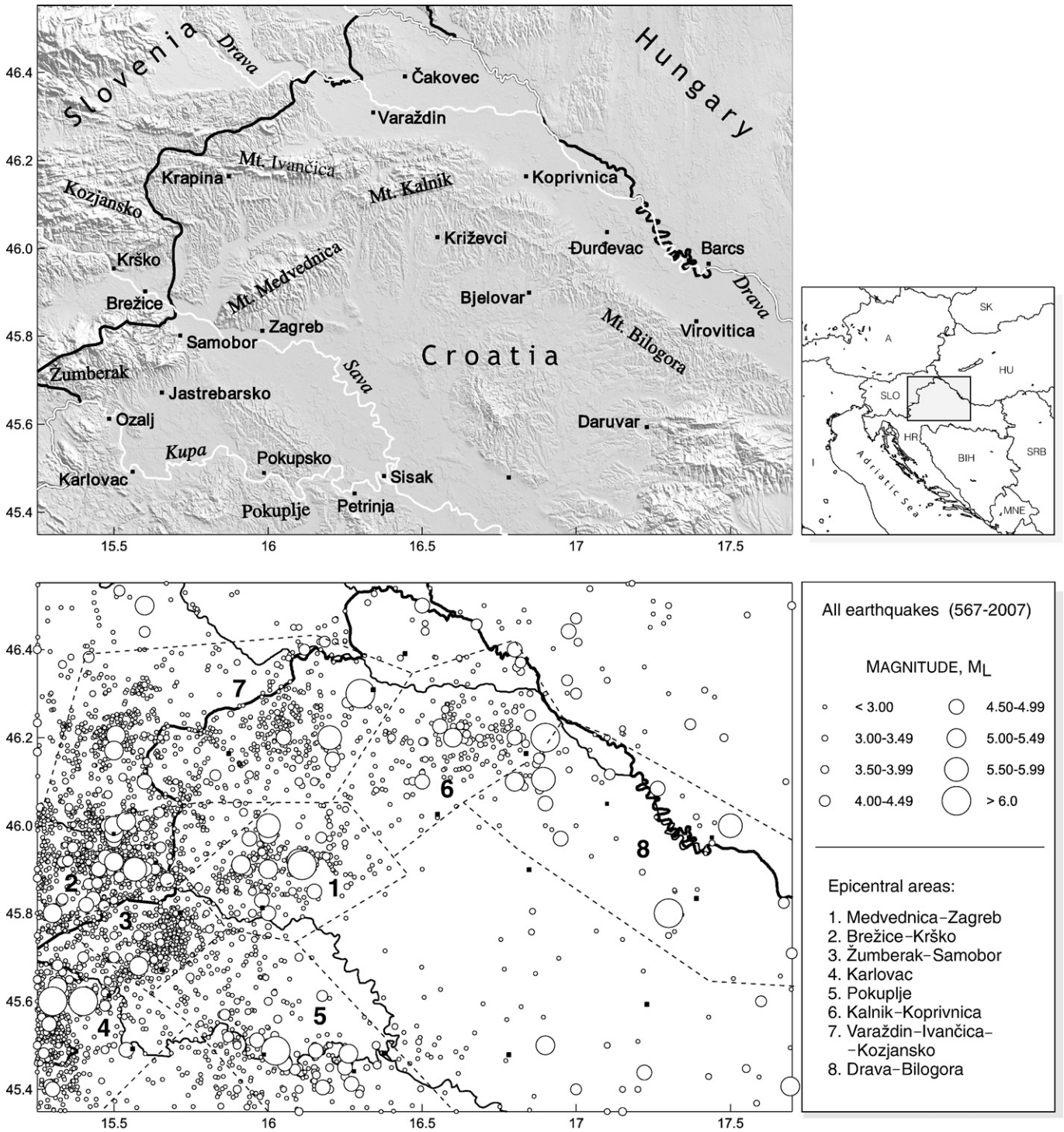


Fig. 1. Top: overview topography map of NW Croatia. Position of the research area is shown by a gray rectangle in a small map to the right. Bottom: Epicentres of all earthquakes (567–2007) reported in the Croatian Earthquake Catalogue in the studied region. Events after 1908 are relocated in the course of this study. Main epicentral areas (dashed lines) are identified by numbers in the legend.

time of update, preliminary locations are obtained using the HYPOSEARCH algorithm (Herak, 1989) and the average, standard model of the crust and upper mantle (BCIS, 1972). Later—typically with a delay of a year or two—all available data are collected, the solutions are recalculated and manually checked by a seismologist. These solutions are further refined only in major catalogue revisions (the second one is under way), or whenever a dedicated seismicity study—like this one—is made. Here, we have re-computed locations of all

events (1908–2007) in two stages. In the first stage, the standard crustal model was gradually refined during four series of earthquake locations followed by the grid search of model parameters that minimize the observed sum of squared residuals of onset times. The second stage consisted of seven iterations involving earthquake locations using the final model obtained in stage one, and station corrections (adjusted in each iteration) for all station-phase pairs for which more than 10 data were reported. The iterations were stopped

Table 1
Earthquakes with available fault-plane solutions (FPS)

No.	Date	Time	Lat °N	Lon °E	<i>h</i> , km	<i>M_L</i>	φ_1°	δ_1°	λ_1°	φ_2°	δ_2°	λ_2°	<i>P_φ</i> °	<i>P_δ</i> °	<i>T_φ</i> °	<i>T_δ</i> °
1	1938-03-27	11:15:59.8	46.105	16.894	03.0	5.6	190	25	142	315	75	70	61	27	200	56
2	1974-06-20	17:08:27.8	46.205	15.506	11.6	5.1	305	58	149	53	64	36	178	4	271	43
3*	1982-03-16	13:52:23.7	46.163	16.210	18.5	4.5	267	38	89	88	52	91	178	7	2	83
4	1984-03-11	11:55:32.3	45.869	15.445	14.2	4.2	326	54	-128	199	50	-49	175	60	82	2
5*	1990-09-03	10:48:32.2	45.911	15.913	13.6	5.0	261	43	94	76	47	86	169	2	302	86
6	1993-05-29	08:43:11.1	45.549	15.289	13.8	4.6	225	43	-7	320	85	-132	194	35	83	27
7*	1993-06-01	19:51:09.8	46.225	16.557	17.8	4.7	93	38	71	296	55	104	16	9	249	76
8	1995-08-25	09:27:20.9	45.407	17.694	18.8	5.0	287	49	71	135	44	111	30	2	129	76
9	1996-09-10	05:09:26.4	45.413	16.271	16.0	4.5	233	49	-8	328	84	-138	199	33	94	23
10	1997-04-30	19:18:18.4	45.930	16.189	15.1	3.8	251	52	13	153	80	141	207	18	105	34
11	1998-06-02	18:02:56.8	46.116	17.109	15.2	4.1	86	45	-165	345	79	-45	294	39	43	22
12	2000-06-16	02:34:58.0	45.924	15.955	14.1	3.7	248	53	52	120	51	129	4	1	96	61
13	2003-08-02	20:31:48.0	45.894	17.215	24.5	3.5	259	61	-28	3	66	-147	223	39	130	3
14	2004-01-08	14:23:31.4	45.873	15.975	13.8	2.4	103	32	34	343	73	117	53	23	287	54
15	2005-12-07	05:22:02.6	46.191	16.501	18.3	3.6	243	43	60	101	54	115	174	6	69	69
16	2006-01-08	15:22:33.8	45.490	16.168	15.9	3.5	91	75	50	344	42	157	210	20	321	45
17	2006-01-23	21:29:04.4	45.776	15.721	12.9	3.6	47	88	5	317	85	178	182	2	272	5
18	2006-04-10	08:35:21.6	46.207	15.441	14.2	2.7	312	64	-155	210	68	-27	170	35	262	2
19	2006-07-19	02:34:05.9	45.695	15.629	14.6	3.5	104	62	-155	2	68	-29	321	37	54	4
20	2006-10-28	13:55:29.8	45.734	15.651	15.0	3.9	22	79	-31	119	60	-166	336	29	74	13
21	2007-04-19	11:18:35.5	46.196	15.518	11.9	2.8	299	57	82	133	34	102	35	12	184	77
22	2008-03-05	19:41:24.6	45.769	15.936	16.6	3.1	145	57	173	239	84	33	7	18	107	27

φ , δ , λ are the strike, dip and rake of the two possible fault planes, *P_φ*, *P_δ* are the trend and plunge of the pressure axis, *T_φ*, *T_δ* are the same for the tension axis.

* Earthquakes for which FPS are taken from Pondrelli et al. (2006).

when no station correction changed by more than 0.01 s. The final locations of all events are presented in Fig. 1.

3. Fault-plane solutions

Low seismicity of the area since the second half of the 20th century (only two earthquakes exceeded *M_L*=5.0), combined with a small number of seismological stations working in the neighbourhood until 1990-ies, prevented computation of fault-plane solutions (FPS) for more than just a few events. Herak et al. (1995) published FPS parameters for three earthquakes. Recently, Pondrelli et al. (2006) published the Italian CMT database, which includes also four earth-

quakes from the studied area. The database of Earthquake Mechanisms of the Mediterranean Area (EMMA, Vanucci and Gasperini, 2004), also lists several solutions from the region, but some of them are significantly mislocated. Here, we present newly computed and revised FPS data obtained on the basis of the first motion polarities (Table 1 and Fig. 2). These data show the prevalence of subhorizontal to moderately dipping *P*-axis, predominantly N–S directed in the central part, to NW–SE and NE–SW directed in the western and eastern parts of studied area, respectively. They indicate the compressional stress field in the central part of the studied area, which promotes dip-slip movements along reverse E–W striking faults versus transpressional stress field in the western and eastern

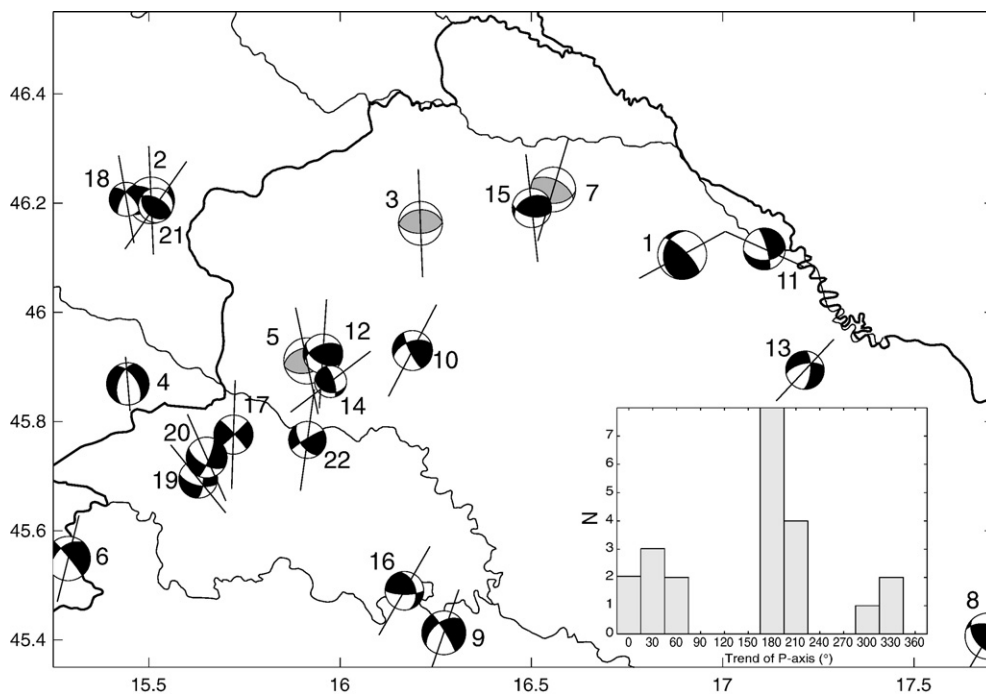


Fig. 2. Lower hemisphere equal area projections of the fault-plane solutions listed in Table 1. Compressional first motions quadrants are black (or gray for solutions from Pondrelli et al., 2006). The beach-balls' radius is scaled with magnitude. The bars are in direction of the *P*-axis, their length being proportional to its horizontal projection. The number adjacent to each earthquake corresponds to numbers in Table 1. The histogram in the inset shows distribution of *P*-axis trends (clockwise from N).

sectors that is accommodated by strike-slip motions. This is in agreement with measurements and calculations of Quaternary stress field in the area obtained by different methods (Prelogović et al., 1998; Bada, 1999; Tomljenović and Csontos, 2001 and references therein).

4. Historical seismicity in the light of tectonics and focal-mechanism solutions

The account of historical seismicity heavily relies on reports by Kišpatić (1888, 1891, 1892, 1905, 1907) and Ribarič (1982) who identified a number of strong earthquakes with epicentral intensities up to IX °MCS. Some of them, unfortunately, are quite uncertain, being based on unreliable historical sources (e.g. 567 near Karlovac, 1459 near Varaždin, or the notoriously suspicious earthquake of 1502 near Zagreb which was eventually removed from the catalogue—see e.g. Cčić et al., 1998). Throughout this section we'll cite intensities in the scale as originally reported in our archives. In most cases this is the Mercalli-Cancani-Sieberg (MCS) scale.

The *Medvednica-Zagreb area* experienced strong seismic activity in the 18th, 19th and in the beginning of the 20th century. The strongest earthquakes occurred on 13 October 1775 with the epicentral intensity of VII–VIII °MCS (destroyed a church in Bedekovčina), on 9 November 1880 with the intensity VIII °MCS, on 17 December 1905 (I_0 =VII–VIII °MCS) and on 2 January 1906 (I_0 =VII–VIII °MCS). The great Zagreb earthquake of 1880 is very well documented (Torbar, 1882), due to efforts of the Earthquake Committee founded by the Academy immediately after the earthquake. This is the first Croatian earthquake for which focal depth (16 km) was ever estimated based on macroseismic and other observations. Of 3670 buildings (Zagreb had only 30,000 inhabitants!), all were damaged and about 13% were destroyed. The epicentre of this event was in the village of Planina, about 17 km to the north-east of Zagreb, where almost all masonry buildings were destroyed. The phenomenon of liquefaction (including mud volcanoes) was observed in the villages that lay in the valley of the Sava River. The earthquake was felt over a very wide area (e.g. in Dubrovnik, 397 km away). This is one of the most important Croatian earthquakes which practically defines the lower hazard bounds in the Zagreb metropolitan area. The epicentres of the 1905 and 1906 events most probably coincided with the one of the great Zagreb earthquake of 1880. Again almost all houses were destroyed in the Planina village (Kišpatić, 1905, 1907). Heavy damage occurred also in Čučerje, Vugrovec and Kašina (some 15 km NE from Zagreb downtown), where churches and many houses were ruined (Mohorovičić, 1908). These earthquakes prompted local authorities to finance installation of the Vicentini-Konkoly seismograph in Zagreb (Herak and Herak, 2007), thus founding the Zagreb seismological station. According to recent seismicity the seismogenic layers extend to depths of about 16 km. All felt events occurred below 6 km. Calculated and available fault-plane solutions (FPS No. 5, 10, 12, 14 and 22, Table 1; Fig. 2) indicate seismogenic activity on (1) reverse ENE–WSW striking faults and (2) along dextral or sinistral NW–SE and ENE–WSW striking faults, respectively. The hypocentres in the western part of this area lie in a steeply SSE-dipping zone (profiles A–B in Fig. 3) in agreement with the Quaternary active SE-dipping reverse fault mapped along the northern margin of Mt. Medvednica (Fig. 1; see Fig. 3 in Tomljenović et al., 2008 for a map and profile view of this fault). This fault nicely corresponds in orientation and kinematics with the NE–SW striking and SE-dipping nodal plane of FPS No. 5 (Table 1; Fig. 2) indicating reverse, top-to-the-NW hangingwall motion direction. Two FPS (No. 10 and 22; Table 1, Fig. 2) related to earthquakes in the northeastern and southwestern parts of this epicentral area indicate seismogenic structures corresponding either to the NW–SE striking dextral or the NE–SW striking sinistral faults. In both cases, the first option is more plausible because it is in quite good agreement with the location,

orientation and kinematics of two NW–SE striking dextral faults mapped in this area (see Fig. 2 in Tomljenović and Csontos, 2001 and Fig. 3 in Tomljenović et al., 2008).

In the *Brežice-Krško area* three strong earthquakes are reported. On 17 June 1628 an earthquake with the estimated intensity of VIII °MCS occurred in the Krško-Brestanica area. According to Ribarič (1982) many castles, churches and other buildings were ruined. The Ribarič catalog also reports the earthquake of intensity IX °MCS in 1640 in the Brežice area, but without any details. The 1917 (29 January) earthquake (I_0 =VIII °MCS, M_L =5.7) occurred in the region Brežice–Krška vas–Globoko–Stojdraga, causing great damage to the Brežice castle. Ribarič (1982) also cites several earthquakes with I_0 =VII °MCS in the years 1632, 1830, 1853, 1924, and 1928.

The epicentral area of *Žumberak-Samobor* experienced the strongest known earthquake on 11 February 1699. According to Ribarič (1982) the town of Metlika (Slovenia) suffered extensive damage, with ruined buildings and human losses. The earthquake of 13 August 1887 (I_0 =VII °MCS) caused heavy damage on churches and houses in Jastrebarsko and the surrounding villages of St. Jana, Krašič, and Slavetić. Some damage was also reported in Metlika (Kišpatić, 1888). This earthquake was felt strongly along 80 km distance from Karlovac to Krapina and in the border region between Croatia and Slovenia. The three fault-plane solutions calculated for this region (FPS No. 17, 19 and 20; Table 1, Fig. 2) point to the prevalence of strike-slip tectonics accommodated by steeply dipping NE–SW striking sinistral and/or NW–SE striking dextral fault sets. A steeply SSE-dipping seismogenic zone is also depicted by hypocentres in a section across this epicentral area (cross sections E–F in Fig. 3). Post-Neogene transpressional tectonics under generally N–S trending greatest principal stress direction is also evidenced by structural data obtained from surface and subsurface (reflection seismic surveying), which indicate the youngest movements along the southern margin of Mt. Žumberak accommodated by sinistral NE–SW striking fault set (Tomljenović, 2002).

The *Karlovac epicentral area* did not exhibit pronounced seismicity in recent centuries. Only one event (14 June 1853) reached intensity VI °MCS. Old historical documents, however, report about strong earthquakes in 1645 and 1646, which nearly completely destroyed fortification walls in the town of Karlovac (Kišpatić, 1892). One FPS calculated from earthquake on the Croatian-Slovenian border (No. 6, Table 1, Fig. 2) indicates NNE–SSW directed pressure axis and oblique-slip motion either on dextral NW–SE striking or sinistral NE–SW striking fault. According to fault traces and strike of Plio-Quaternary basins presented on geological map of this area (Bukovac et al., 1983), the former seems more probable as the earthquake generating fault.

The *epicentral area of Pokuplje* lies along the Kupa River, between Karlovac and Sisak. No account of strong earthquakes before the 19th century exists there. The first known event to have exceeded an intensity of VII °MCS occurred on 18 December 1861 (Kišpatić, 1892). The most important, however, is the one of 8 October 1909 (M =6.0, I_0 =VIII °MCS), the well-known earthquake with the epicentre near the village of Pokupsko, about 40 km SE of Zagreb. Brick and stone masonry buildings were considerably damaged, but there was no damage to wooden (oak) frame houses. Epicentral area is elongated NW–SE, with maximal effects in the villages of Kupinec, Pokupsko, Brest Pokupski, Donja Bučica, Šišinec, Glina, Gora, Farkašič, Mala Solina, and Stankovac. The earthquake was also strongly felt in Zagreb, where a number of chimneys toppled. Liquefaction was widely reported in the Kupa valley. Field reports also mention large fluctuations of the groundwater level in wells (Herak et al., 1996; Mohorovičić, 1910). The strongest aftershock (28 January 1910, M_L =5.3, I_0 =VII–VIII °MCS) heavily damaged buildings in the epicentral area (Farkašič, Gora, Petrinja, Martinska Ves, Glina). Two FPS available from this area (No. 9 and 16, Table 1, Fig. 2) consistently indicate a moderately plunging SW-trending pressure axis, with potential earthquake generating fault corresponding

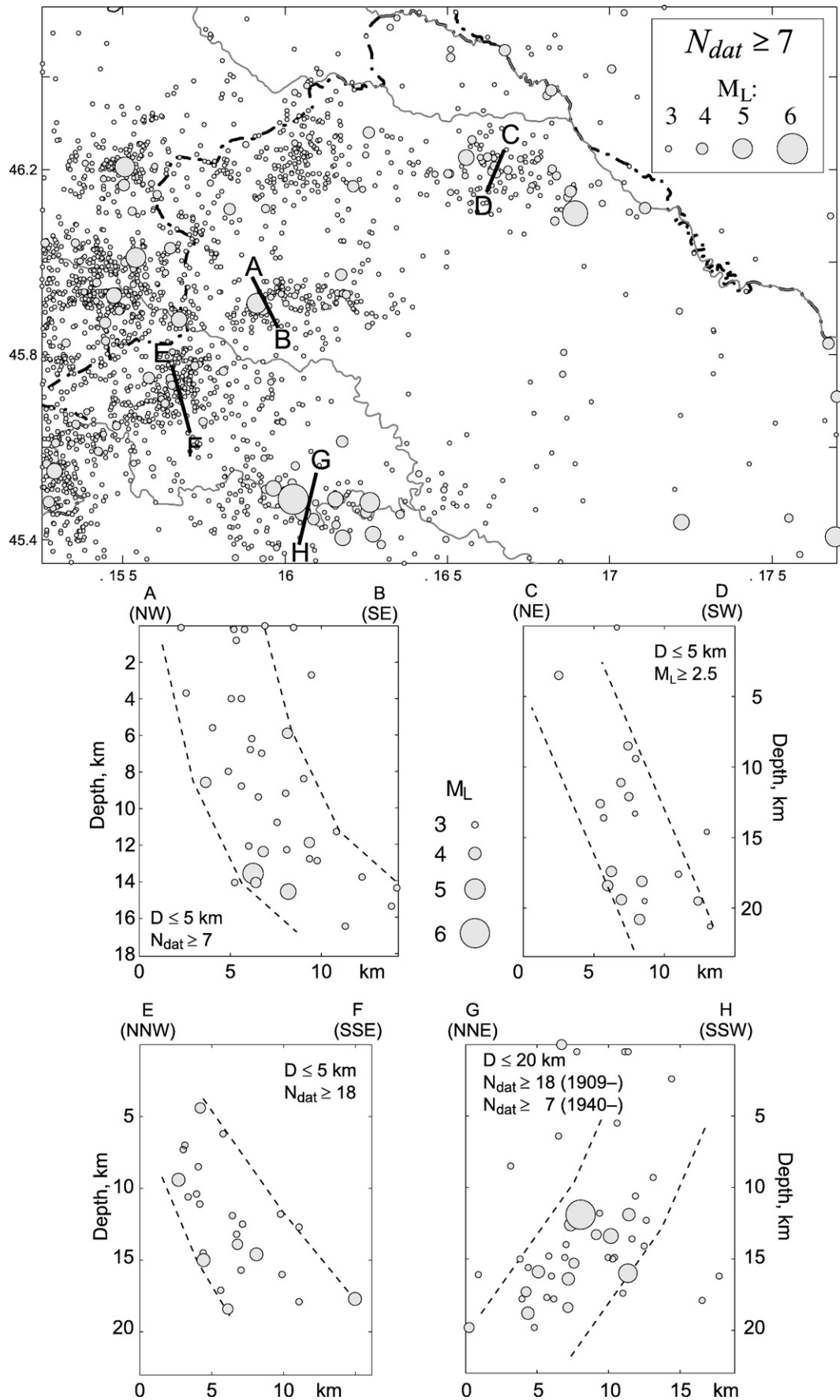


Fig. 3. Top: epicentres of all relocated events for which at least 7 onset times were reported. Typical computed uncertainties ($\pm 1\sigma$) for horizontal coordinates are smaller than 3 km, whereas the average uncertainty of depth is about twice as large. *Middle and bottom:* vertical cross-sections along the lines shown in the map. D denotes maximal allowed distance from the profile, N_{dat} is number of onset times used to locate earthquakes, and M_L is local magnitude. Dashed lines are drawn only to enhance trends and have no direct geological interpretation.

either to NW–SE striking dextral or NE–SW striking sinistral fault set. Based on the fault map of Prelogović et al. (1998) the former seems more plausible and would be a part of the Sava fault zone, which is seen as the NE-dipping boundary normal fault zone along the southwestern margin of the Pannonian basin during the Neogene. At present, however, this fault zone would be reactivated and inverted, accommodating dextral and reverse motions due to recently NE–SW directed compression in this region. This interpretation is additionally supported by a cross-sectional view of hypocentres indicating a seismogenic zone which dips due NE with an angle of 60° that is typical for normal faults (Fig. 3, profiles G–H). Strong events are concentrated at focal depths between 10 and 20 km.

The Kalnik–Koprivnica epicentral area is known to have experienced only moderate seismicity with macroseismic intensity up to VII °MCS (20 December 1883, and 1 June 1993). Both events occurred near the town of Koprivnica. The 1993 earthquake was widely felt in the north-western part of Croatia, in the western part of Slovenia and in the border areas of Hungary and Austria. The maximum intensity of VII °MSK was reported in the villages of Duga Reka, Radljevo and Ribnjak. Two FPS from this area (No. 7 and 15, Table 1, Fig. 2) as well as cross-sections C–D in Fig. 3 indicate seismogenic faulting on E–W to NW–SE striking reverse faults dipping to the S–SW, which is in a good agreement with faults of practically the same orientation and kinematics mapped along the northern margin of the Mt. Kalnik (Prelogović et al., 1998).

Although recent seismicity indicates considerable activity of the Varaždin–Ivančica–Kozjansko epicentral area, only very doubtful data exist on historical earthquakes there (e.g. the 1459 earthquake near Varaždin, $I_0 = IX$ °MCS). The 12 November 1836 ($I_0 = VII$ –VIII °MCS) earthquake damaged the village of Zajezda (Kišpatić, 1891). A strong earthquake in the Slovenian part of the area badly damaged the Podčetrtek castle on 20 June 1974 ($M = 5.1$, $I_0 = VII$ –VIII °MCS) (Ribarič, 1982; Zorn and Komac, 2004). It was felt over the whole Kozjansko region in Slovenia (Šmarje pri Jelšah, Šentjur pri Celju, Celje, Slovenske Konjice) where 15% of buildings were ruined. The event triggered extensive landslides and rockfalls. One FPS from the eastern part of this area reported by Pondrelli et al. (2006) indicate compressional tectonics with N–S trending P -axis and dip-slip reverse motion along E–W striking nodal planes, all in good agreement with the E–W striking pop-up structure of Mt. Ivančica and stress calculations from fault-slip data (Tomljenović and Csontos, 2001; Prelogović et al., 1998). The three focal mechanisms of events in Slovenia (Kozjansko) also reveal a predominantly N–S directed compression.

The Drava–Bilogora epicentral area extends for about 75 km between towns of Koprivnica and Virovitica. Three of four earthquakes with $I_0 \geq VII$ °MCS that are known from this area had epicentres near Koprivnica. The first event (25 May 1694) has an assigned intensity of VII °MCS. The strong earthquake ($I_0 = VIII$ °MCS) of 8 November 1778 caused heavy damage in Koprivnica and Legrad and their vicinity (Kišpatić, 1891). The 27 March 1938 earthquake ($I_0 = VIII$ °MCS) destroyed many houses and churches in the town of Đurđevac and the villages of Novigrad Podravski and Kapela. Heavy damage was also reported on houses in Veliko Trojstvo, Severin, Virje and Virovitica. This is the first event in Croatia for which a fault-plane solution could have been computed (No. 1, Table 1, Fig. 2). Probable seismogenic structure is the NW–SE striking fault dipping at 75° due NE. This would correspond to the major NW–SE striking oblique-slip fault mapped by Prelogović et al. (1998). The earthquake of 8 July 1757 ($I_0 = VIII$ °MCS) occurred beneath Mt. Bilogora close to Virovitica. This event caused widespread damage on masonry buildings in Virovitica and its neighbourhood. Many cracks which appeared in the ground were filled with water and yellow sand. It was also reported that wells overflowed (Kišpatić, 1891). Two important earthquakes with intensity $I_0 \geq VII$ °MCS occurred in the Drava River valley in the Croatia–Hungary border region. The first one (12 July 1836, $I_0 = VII$ –VIII °MCS) caused damage near the town of

Barcs (Hungary), and the second one with $I_0 = VII$ °MCS occurred west of Barcs in 1927 (Zsiros et al., 1988).

5. Catalogue completeness and declustering

The catalogue compiled as described above, supplemented by its historical part (prior to 1908) serves as the basic database for all subsequent analyses, most notably for seismic hazard studies. It is then of utmost importance to reliably estimate magnitude completeness thresholds for various time periods. However, the area considered in this study is also spatially quite heterogeneous, not just considering the seismicity level, but also the historical coverage by seismological stations, the amount of research done, etc. This eventually resulted in considerable spatial heterogeneity of the catalogue, as far as completeness is concerned. To the best of our knowledge, no method of estimating the completeness of an earthquake catalogue is the standard one. Usually, catalogues are considered complete for times $t > t_c$ and magnitudes $M \geq M_c$ if some quantity describing earthquake recurrence (e.g. the Gutenberg–Richter b -value) ‘stabilizes’ after t_c (considering all events with $M \geq M_c$). The change in slope of the frequency-magnitude relation was used to assess M_c by e.g. Wiemer and Wyss (2000), Rydelek and Sacks (1989) used changes between the day and night-time sensitivity of networks, whereas Gombert (1991) utilize amplitude threshold studies. The later two methods are deemed too complicated, time-consuming and not general enough to be used in a study like this one. The techniques that rely on the assumption of log-linearity of the magnitude distribution (constant b -value) require rather large datasets to attain stability, which is in our case difficult to achieve because of relatively low seismicity and the need to consider also short time-windows. Therefore we choose the rate of earthquake occurrence as determining quantity, and define t_c as the time when the cumulative activity rate (A_c) first reached the ‘true’ average activity rate, A_0 . A_c is a function of the threshold magnitude, M_c , and the time:

$$A_c(M_c, t_c) = N(M \geq M_c, t > t_c) / (t_{last} - t_c), \quad (1)$$

where N is the number of earthquakes in the catalogue with the magnitude larger than M_c and which have occurred after t_c (t_{last} is the time of the last earthquake in the catalogue, usually close to the present time). The problem is, of course, how to define A_0 , or the

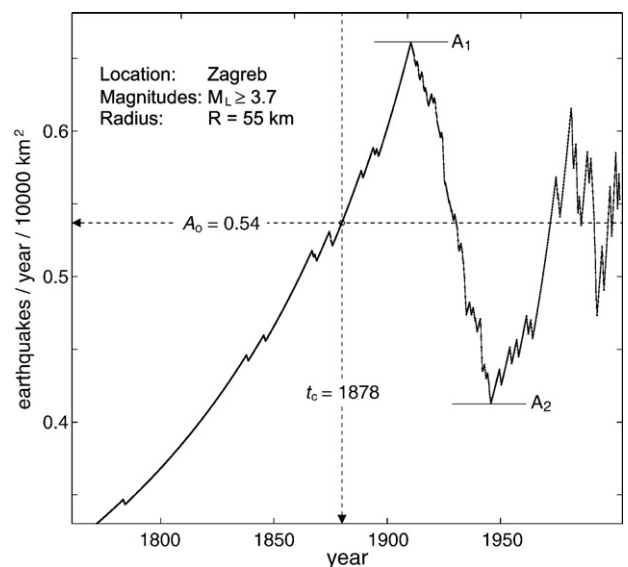


Fig. 4. Cumulative activity rate of earthquakes with magnitudes $M_L \geq 3.7$ in a circle with radius of 55 km around the city of Zagreb as function of time (Eq. (1)). The curve is computed for discrete times corresponding to times of occurrence of all events in a declustered catalogue (mainshocks only).

Table 2
Windowing parameters used to decluster the catalogue

M_L	D_w (km)	T_w (days)	T_w (years)	M_L	D_w (km)	T_w (days)	T_w (years)
3.0	10.0	15.0	0.0411	5.2	30.3	127.1	0.3479
3.2	11.1	18.2	0.0499	5.4	33.5	154.3	0.4225
3.4	12.2	22.1	0.0606	5.6	37.1	187.4	0.5131
3.6	13.5	26.9	0.0736	5.8	41.0	227.6	0.6231
3.8	15.0	32.6	0.0893	6.0	45.3	276.4	0.7567
4.0	16.5	39.6	0.1085	6.2	50.1	335.6	0.9189
4.2	18.3	48.1	0.1317	6.4	55.4	407.6	1.1160
4.4	20.2	58.4	0.1600	6.6	61.3	495.0	1.3552
4.6	22.4	71.0	0.1943	6.8	67.8	601.1	1.6458
4.8	24.8	86.2	0.2359	7.0	75.0	730.0	2.0000
5.0	27.4	104.6	0.2865				

$\min(D_w)=10.0$ km, $\min(T_w)=10.0$ days, $T_{w, aft}/T_{w, for}=5.0$

For $M_L < 3.0$ and $M_L > 7.0$, the parameters are estimated by log-linear extrapolation. D_w —radius of circular window; T_w , $T_{w, aft}$ —duration of aftershocks; $T_{w, for}$ —duration of foreshocks.

reference ('true') activity level. Again, there is no prescribed path to follow, but if it is reasonable to assume that the most recent data above certain magnitude are practically complete, we may choose to define A_0 on this basis. The curve $A_c(M_c, t)$ versus t is always characterized by a steady increase as the catalogue gets more complete. When complete reporting is achieved, it stabilizes, and oscillates around the value of A_0 for the rest of time until present. The oscillations are due to natural (aleatory) variation of seismicity, but will also appear close to t_{last} when neither N nor $(t_{last} - t_c)$ in Eq. (1) are large enough to keep the ratio stable. We therefore stop the analysis at time when N falls below $N = 30/M_c$. This is an arbitrary threshold, but seems to produce reasonable results. If the total number of earthquakes with $M \geq M_c$ is lower than N (typically for large M_c only), the year of the beginning of complete reporting is conservatively determined by a seismologist's educated guess. We define A_0 as the mean level between the maximum value of A_c achieved (A_1 in Fig. 4) and the absolute minimum of A_c after the maximum (A_2 in Fig. 4). Fig. 4 shows an example for the case of the circular window of 55 km radius around the city of Zagreb. Following the approach described above, we estimate the declustered catalogue (mainshocks only) to be complete for magnitudes $M_L \geq 3.7$ since 1878—very close to 1880, the year of the

great Zagreb earthquake, when systematic collection of earthquake related data began in this part of Croatia.

Declustering itself has been done using the temporal and spatial windows whose size increased with the mainshock magnitude according to Table 2. All events occurring within time T_w after the mainshock, and within D_w km from its epicentre were declared aftershocks, and were removed from the catalogue. The foreshocks were identified using the same spatial windows, but with 5 times shorter temporal span. The particular window sizes used are the result of experience in years of analyses of Croatian seismicity. They are intermediate between the values suggested by Gardner and Knopoff (1974) and Knopoff (2000), and turned out to produce the mainshock catalogues whose complete parts are Poissonian at least on the 0.95 level of significance when tested by the Anderson-Darling or the χ^2 -tests.

Repeating the completeness analyses for other threshold magnitudes, we obtain the 'staircase' graph as shown left in Fig. 5. Knowing the completeness interval for each magnitude class, the b -value and the normalized reference activity rate (A_r) in the Gutenberg-Richter recurrence relationship

$$\log A = \log A_r - b(M - M_r) \quad (2)$$

can be estimated by the maximum-likelihood method using the algorithm proposed by Weichert (1980) (Fig. 5, right). In Eq. (2), A is the activity rate, i.e. the annual number of earthquakes per standard area (equal here to 10,000 km²) with magnitudes greater or equal to M , M_r is the arbitrarily chosen reference magnitude ($M_r = 3.5$ here), and A_r is the corresponding activity rate.

The same procedure was applied to every node in a dense network (11 × 11 km) covering the whole area under study. In order to ensure large enough number of earthquakes within each circular window during computation of recurrence parameters, its radius was allowed to vary between 30 and 70 km, until it contained at least 50 earthquakes within their respective time interval of complete reporting.

Fig. 6 displays examples of maps showing spatial variation of the catalogue completeness. Fig. 6a shows estimated magnitude completeness thresholds for the year 1950. While in the west M_c is

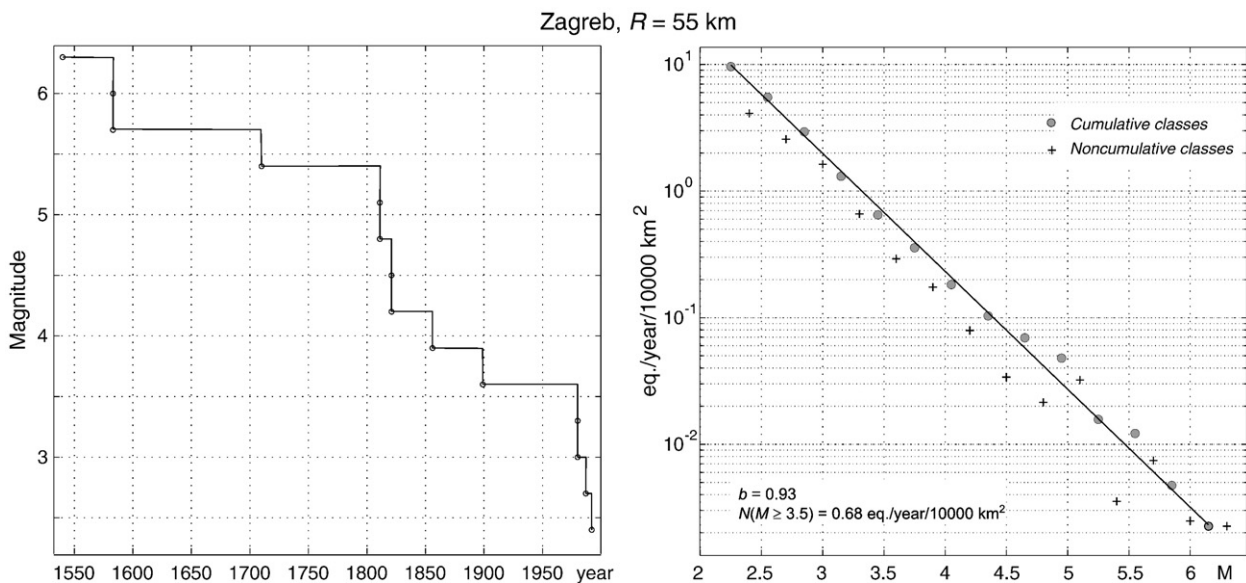


Fig. 5. Left: 'staircase' graph with estimated times of beginning of complete reporting for a subcatalogue of mainshocks with $M_L \geq 3.7$ and epicentral distance to Zagreb less than 55 km. Right: observed cumulative (circles) and noncumulative (crosses) frequencies (55 km around Zagreb, normalized to one year and the area of 10,000 km²). The best fit Gutenberg-Richter frequency-magnitude distribution computed after Weichert (1980) taking unequal observation intervals for each magnitude class (from the subplot on the left) into account is shown by a full line.

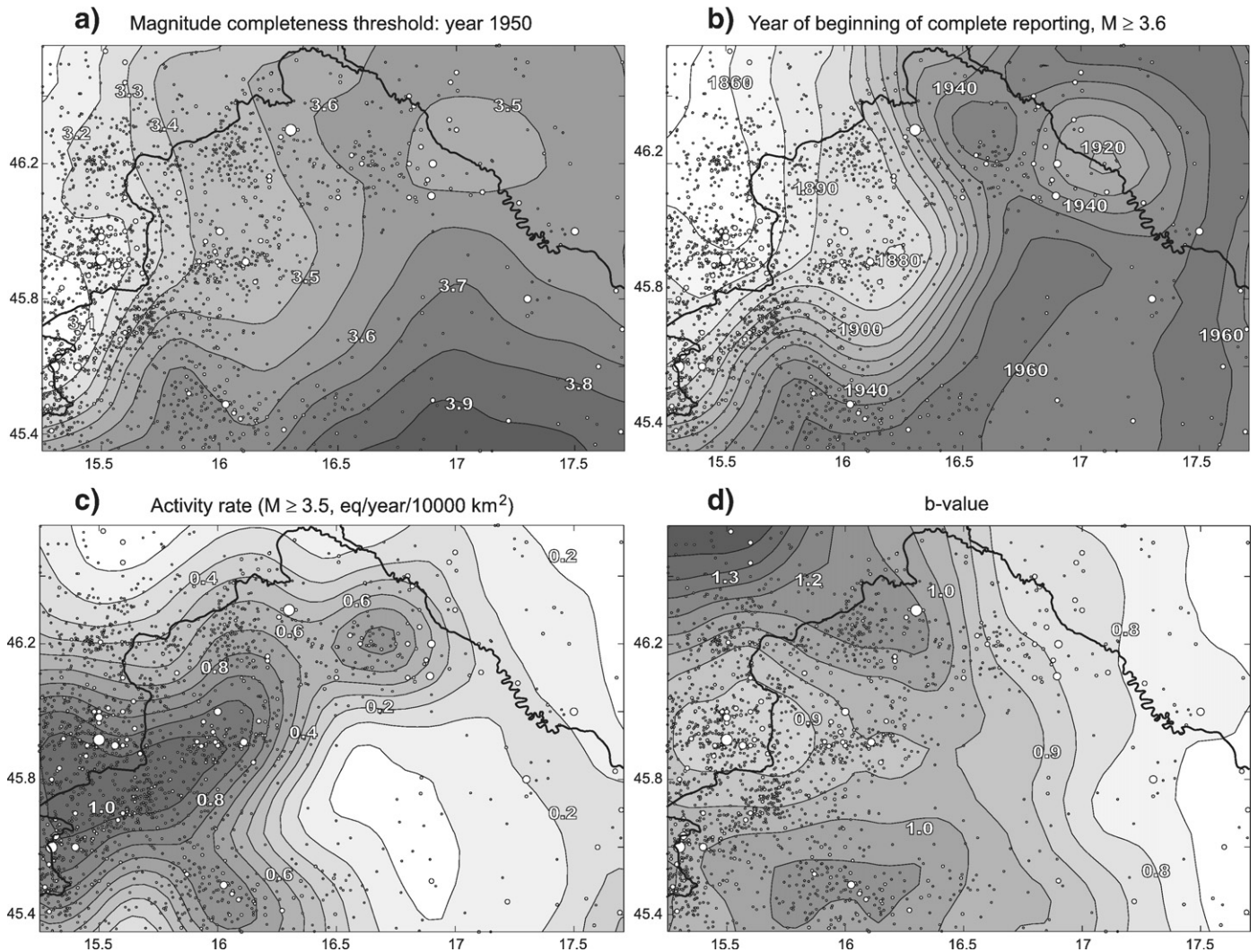


Fig. 6. a) Spatial variation of estimated magnitude completeness for the year 1950; b) spatial distribution of estimated year of the beginning of complete reporting for magnitudes $M_L \geq 3.6$; c) activity rate for $M_L \geq 3.5$ in the Gutenberg-Richter magnitude-frequency distribution, normalized to 10,000 km²; d) estimated slope (b -value) of the magnitude-frequency relationship.

between 3.1 and 3.2, in the southernmost parts it is as high as 3.9. A similar picture is seen if M_c is fixed to $M_c = 3.6$ (Fig. 6b). The observed completeness pattern is determined mostly by the density of population and the degree of development in the last decades of the 19th and in the first half of the 20th century, so that the estimated year of the beginning of complete reporting spreads through a whole century!

Based on results like the ones presented in Fig. 6b we then estimated the Gutenberg-Richter recurrence law (Eq.(2)) for each grid point, and compiled maps of the activity rate (expressed as the average annual number of earthquakes with $M_L \geq 3.5$ per 10000 km²) and the b -value (Fig. 6c and d, respectively). The most active part is the one stretching from the Brežice–Krško epicentral area towards the Zagreb–Medvednica zone. The b -value takes mostly 'normal' values between 0.8 and 1.2, and is not correlated with the activity rate (coefficient of determination $r^2 = 0.02$).

6. Conclusions

We have presented an account of the seismicity of NW Croatia, seismically the most vulnerable part of the country. It is based on historical sources as well as on the updated part of the Croatian Earthquake Catalogue, in which events occurring after 1908 have been

relocated using adjusted velocity models, station corrections and the revised sets of onset times of seismic phases. The improved picture of the distribution of seismicity shows consistent grouping of foci in space. The FPS database has been enlarged from only three solutions published by Herak et al. (1995) to 22 (of which all but three have been computed in this study). The earthquake mechanisms consistently reveal the subhorizontal to moderately dipping P -axis, predominantly N–S directed in the central part of studied area, to NW–SE and NE–SW directed in the western and eastern parts, respectively. They indicate the prevalence of compressional tectonics with reverse faulting in the central part versus strike-slip motion in the western and eastern sectors. These data are in agreement with stress calculations and kinematics of Quaternary structures obtained by geological studies. The improved locations of hypocentres, together with the FPS database will hopefully enable a more precise correlation of hypocentres to particular fault sets (Tomljenović et al., manuscript in preparation), and will serve as primary seismological data source for the subsequent study of seismogenic faults in the area.

The revised earthquake catalogue, with the estimated spatial variation of completeness levels of mainshocks as presented here may serve as the starting point for site-specific and regional hazard studies. In fact, maps like the ones shown in Fig. 6, accompanied by a map of maximum possible magnitudes, can readily be used as input to seismic

hazard analyses using the smoothed seismicity approach (e.g. Frankel, 1995; Frankel et al., 2000, Lapajne et al., 2003). For non-profit purposes, the catalogue is available by request from the corresponding author.

Acknowledgments

We thank two anonymous referees for their constructive remarks on the manuscript. The study was financed by the Ministry of Science, Education and Sports of the Republic of Croatia, through Projects Nos. 119-1193086-1314, 119-1193086-1315, and 195-1951293-3155. All support is gratefully acknowledged.

References

- Bada, G., 1999. Cenozoic stress field evolution in the Pannonian basin and surrounding orogens. Inferences from kinematic indicators and finite element stress modelling. PhD thesis, Vrije Universiteit, Amsterdam, 204 pp.
- B.C.I.S., 1972. Tables des temps des ondes sismiques. Hodochrones pour la region des Balkans, (Manuel d'utilisation). Strasbourg.
- Bukovac, J., Šušnjar, M., Poljak, M., Čakalo, M., 1983. Basic geological map of Yugoslavia, 1:100.000, sheet Črnomelj. Federal Geol. Institute, Beograd.
- Cecić, I., Sović, I., Živčić, M., 1998. The Zagreb 1502 earthquake—doubtful or even fake? *Annals Geophysics* 16 (supp. 1), C136.
- Fodor, L., Jelen, B., Márton, E., Skaberne, D., Car, J., Vrabec, M., 1998. Miocene-Pliocene tectonic evolution of the Slovenian Periadriatic fault: implications for Alpine-Carpathian extrusion models. *Tectonics* 17, 690–709.
- Frankel, A., 1995. Mapping seismic hazard in the central and eastern United States. *Seismological Research Letters* 66, 8–21.
- Frankel, A., Mueller, C., Barnhard, T., Leyendecker, E., Wesson, R., Harmsen, S., Klein, F., Perkins, D., Dickam, N., Hanson, S., Hopper, M., 2000. USGS national seismic hazard maps. *Earthquake Spectra* 16, 1–20.
- Gardner, J.K., Knopoff, M., 1974. Is the sequence of earthquakes in Southern California, with aftershocks removed, Poissonian? *Bulletin of the Seismological Society of America* 64, 1363–1367.
- Gomberg, J., 1991. Seismicity and detection/location threshold in the southern Great Basin seismic network. *Journal of Geophysical Research* 96, 16401–16414.
- Lapajne, J., Šket Motnikar, B., Zupančič, P., 2003. Probabilistic seismic hazard assessment methodology for distributed seismicity. *Bulletin of the Seismological Society of America* 93 (6), 2502–2515.
- Herak, M., 1989. HYPOSEARCH—an earthquake location program. *Computers & Geosciences* 15, 1157–1162.
- Herak, D., Herak, M., 2007. Andrija Mohorovičić (1857–1936)—on the occasion of the 150th anniversary of his birth. *Seismological Research Letters* 78, 671–674.
- Herak, D., Herak, M., Sović, I., Markušić, S., 1991. Seismicity of Croatia in 1989 and the Kamešnica Mt. earthquake. *Geofizika* 8, 83–99.
- Herak, M., Herak, D., Markušić, S., 1995. Fault plane solutions for earthquakes (1956–1995) in Croatia and neighbouring regions. *Geofizika* 12, 43–56.
- Herak, M., Herak, D., Markušić, S., 1996. Revision of the earthquake catalogue and seismicity of Croatia. *Terra Nova* 8, 86–94.
- Ivančić, I., Herak, D., Markušić, S., Sović, I., Herak, M., 2002. Seismicity of Croatia in the period 1997–2001. *Geofizika* 18/19, 17–29.
- Ivančić, I., Herak, D., Markušić, S., Sović, I., Herak, M., 2006. Seismicity of Croatia in the period 2002–2005. *Geofizika* 23/2, 87–103.
- Kišpačić, M., 1888. Peto izvješće potresnoga odbora za godinu 1887. *Rad Jugoslavenske akademije znanosti i umjetnosti. Matematičko-prirodoslovni razred* 9, 215–227.
- Kišpačić, M., 1891. Potresi u Hrvatskoj. *Rad Jugoslavenske akademije znanosti i umjetnosti. Matematičko-prirodoslovni razred* 13, 81–164.
- Kišpačić, M., 1892. Potresi u Hrvatskoj. *Rad Jugoslavenske akademije znanosti i umjetnosti. Matematičko-prirodoslovni razred* 14, 1–79.
- Kišpačić, M., 1905. Dvadeset i treće potresno izvješće za g. 1905. *Rad Jugoslavenske akademije znanosti i umjetnosti. Matematičko-prirodoslovni razred* 38, 131–180.
- Kišpačić, M., 1907. Dvadeset i četvrto potresno izvješće za prvu četvrt godine 1906. *Rad Jugoslavenske akademije znanosti i umjetnosti. Matematičko-prirodoslovni razred* 41, 1–54.
- Knopoff, L., 2000. The magnitude distribution of declustered earthquakes in Southern California. *Proceedings of the National Academy of Sciences of the United States of America* 97, 11880–11884.
- Magyari, Á., Musitz, B., Csontos, L., Van Vliet-Lanoë, B., 2005. Quaternary neotectonics of the Somogy Hills, Hungary (part I): evidence from field observations. *Tectonophysics* 410, 43–62.
- Markušić, S., Herak, D., Sović, I., Herak, M., 1993. Seismicity of Croatia in the period 1990–1992. *Geofizika* 10, 19–34.
- Markušić, S., Herak, D., Ivančić, I., Sović, I., Herak, M., Prelogović, E., 1998. Seismicity of Croatia in the period 1993–1996 and the Ston-Slano earthquake of 1996. *Geofizika* 15, 83–102.
- Mohorovičić, A., 1908. Godišnje izvješće Zagrebačkoga meteorološkog opservatorija za godinu 1906, Zagreb.
- Mohorovičić, A., 1910. Das beben vom 8. X. 1909., *Jahrbuch des meteorologischen Observatoriums in Zagreb (Agram) fuer das Jahr 1909.* 9/4, 63 pp.
- Pondrelli, S., Salimbeni, S., Ekström, G., Morelli, A., Gasperini, P., Vanucci, G., 2006. The Italian CMT dataset from 1977 to the present. *Physics of the Earth and Planetary Interiors* 159, 286–303.
- Prelogović, E., Saftić, B., Kuk, V., Velić, J., Dragaš, M., Lučić, D., 1998. Tectonic activity in the Croatian part of the Pannonian basin. *Tectonophysics* 297, 283–293.
- Ribarčič, V., 1982. Seismicity of Slovenia, Catalogue of earthquakes (792 A.D.–1981). *Publications of the Seismological Survey of Slovenia. Series A, No. 1-1.*
- Rydelek, P.A., Sacks, I.S., 1989. Testing the completeness of earthquake catalogs and the hypothesis of self-similarity. *Nature* 337, 251–253.
- Tomljenović, B., 2002. Strukturne značajke Medvednice i Samoborskog gorja (in Croatian, translated title: Structural characteristics of Medvednica and Samoborsko gorje Mts.). PhD Thesis, University of Zagreb, Zagreb, 208 pp.
- Tomljenović, B., Csontos, L., 2001. Neogene-Quaternary structures in the border zone between Alps, Dinarides and Pannonian Basin (Hrvatsko Zagorje and Karlovac Basins, Croatia). *International Journal of Earth Sciences* 90, 560–578.
- Tomljenović, B., Csontos, L., Márton, E., Márton, P., 2008. Tectonic evolution of the northwestern Internal Dinarides as constrained by structures and rotation of Medvednica Mountains, North Croatia. In: Siegesmund, S., Fügenschuh, B., Fritzsche, N. (Eds.), *Tectonic Aspects of the Alpine-Dinaride-Carpathian System. Special Publications, vol. 298.* Geological Society, London, pp. 145–167.
- Torbar, J., 1882. Izvješće o Zagrebačkom potresu 9. studenoga 1880, *Rad JAZU, knjiga I, Zagreb.*
- Vanucci, G., Gasperini, P., 2004. The new release of the database of Earthquake Mechanisms of the Mediterranean Area (EMMA Version 2). *Annals of Geophysics* 47 (supp.), 307–334.
- Weichert, D., 1980. Estimation of the earthquake recurrence parameters for unequal observation periods for different magnitudes. *Bulletin of the Seismological Society of America* 70, 1337–1346.
- Wiemer, S., Wyss, M., 2000. Minimum magnitude of completeness in earthquake catalogs: examples from Alaska, the Western United States, and Japan. *Bulletin of the Seismological Society of America* 90, 859–869.
- Zorn, M., Komac, B., 2004. Recent mass movements in Slovenia. In: Orožen Adamič, M. (Ed.), *Slovenia: A Geographical Overview.* Ljubljana: Association of the Geographical Societies of Slovenia. Založba ZRC, pp. 73–80.
- Zsiros, T., Monus, P., Toth, L., 1988. *Hungarian Earthquake Catalog (456–1986).* Hungarian Academy of Sciences, Budapest, 182 pp.